Nanophase-Segregation and Transport in Nafion 117 from Molecular Dynamics Simulations: Effect of Monomeric Sequence

Seung Soon Jang, Valeria Molinero, Tahir Çağın, and William A. Goddard III*

Materials and Process Simulation Center MC 139-74, California Institute of Technology, Pasadena, California 91125

Received: September 23, 2003; In Final Form: January 15, 2004

Nafion polyelectrolyte is widely used in polymer electrolyte membrane fuel cells (PEMFC) due to its high proton conductivity. The properties of hydrated Nafion are attributed to its nanophase-segregated structure in which hydrophilic clusters are embedded in a hydrophobic matrix. However, there has been little characterization of how the monomeric sequence of the Nafion chain affects the nanophase-segregation structure and transport in hydrated Nafion. To study such properties, we carried out molecular dynamics (MD) simulations of Nafion 117 using two extreme monomeric sequences: one very blocky and other very dispersed. Both produce a nanophase-segregated structure with hydrophilic and hydrophobic domains. However, the blocky Nafion leads to a characteristic dimension of phase-segregation that is ∼60% larger than for the dispersed system. We find that the water−polymer interface is heterogeneous, consisting of hydrophilic patches (water contacting sulfonate groups of Nafion) and hydrophobic patches (water contacting fluorocarbon group). The distribution of the hydrophilic and the hydrophobic patches at the interface (i.e., the heterogeneity of interface) is much more segregated for blocky Nafion. This leads to a water diffusion coefficient for the dispersed case that is ∼25% smaller than for the blocky case (0.46×10^{-5} vs 0.59×10^{-5} cm^2/s at 300 K). The experimental value (0.50×10^{-5} cm^2/s) is within the calculated range. On the other hand, we find that the vehicular diffusion of hydronium is not affected significantly by the monomeric sequence. These results should be useful in optimizing the properties of Nafion and as targets for developing other membranes to replace Nafion in PEMFC and other applications.

1. Introduction

Nafion is a polyelectrolyte consisting of nonpolar tetrafluoroethylene (TFE) segments, N = (CF_2-CF_2) and polar perfluorosulfonic vinyl ether (PSVE) segments, P = ($CF_2-CF(O-CF_2-CF(CF_3))-CF_2-CF_2-SO_3H$) (Figure 1) used in many important applications.[1] Particularly of interest to us are the properties relevant to polymer electrolyte membrane fuel cells (PEMFC) where its high proton conductivity and mechanical, chemical, and thermal stabilities are crucial.[2−6] There is a general consensus supported by experiments[7−22] and simulation[23−25] that these favorable characteristics of hydrated Nafion result from its nanophase-segregated structure in which hydrophilic clusters are embedded in hydrophobic matrix.

Various models have emerged to explain the properties of hydrated Nafion membrane[11−13,26−30] since Eisenberg[7] suggested the concept of cluster formation for ionomers, which was extended by Mauritz and Hopfinger[26] in an attempt to represent the structural incorporation of water and ions by introducing configurational dipole−dipole interactions.

One widely accepted empirical model for hydrated Nafion is the cluster−network model proposed by Hsu and Gierke[11,12] on the basis of small-angle X-ray scattering (SAXS) experiments. In this model, spherical hydrophilic clusters (∼4 nm diameter) of water are surrounded by sulfonate groups connected through cylindrical channels with ∼1 nm diameter. They conjectured that the balance between elastic deformation energy and hydrophilic surface interactions leads to these characteristic dimensions.

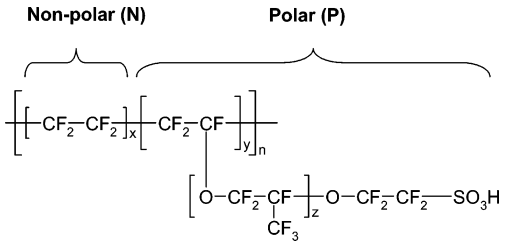

Figure 1. Chemical structure of Nafion. Nafion 117 has an average composition of $x = 6.5$, $y = 1$, and $z = 1$. N indicates for the nonpolar monomeric units while P indicates the polar monomeric units.

Tovbin and Vasyatkin[31,32] used spectroscopic data to suggest a three-dimensional model of the amorphous part of the Nafion membrane as consisting of an ensemble of pores formed by closely packed polymer chains. In this empirical model, the walls of the pores are postulated to consist of polymer bilayers, with the sulfonate groups pointing inward toward the water channels.

To rationalize the observed transport phenomena, Yeager and Steck[13] proposed a "three-phase model" consisting of the fluorocarbon phase (some of which would be microcrystalline), an interfacial region rich in free volume that contains the pendant chains, and the cluster region containing water and ionic groups. The clusters in this model are assumed to be spherical.

It is generally understood that proton transport is strongly coupled with the distribution and transport of water in the hydrated Nafion membrane:

(i) Proton conductivity in PEMFCs is possible only in the presence of water and thus a water-polymer structure with percolation in three dimensions is essential.

* To whom correspondence should be addressed. wag@wag.caltech.edu.

10.1021/jp036842c CCC: $27.50
Published on Web 02/17/2004

(ii) Water transport in Nafion membranes can occur through two mechanisms for the percolated structure:

- diffusion caused by concentration gradient between cathode and anode arising from the water generated at the cathode via O_2 reduction with protons;
- electro-osmotic drag of water by the protons from anode to cathode when the fuel cell is under a bias potential. This mechanism may result in the depletion of water at the anode, which diminishes the proton conductivity by removing the media for proton transfer.

Consequently water transport in hydrated Nafion membrane of fuel cell has been studied intensively using experimental techniques such as radiotracers,[14,33−35] and pulsed field gradient spin−echo ^{1}H NMR.[36−38] However, there have been few attempts to understand the transport phenomena in PEMFC as a function of the nanostructure of the membrane.[18,39−42] This is probably because of the lack of synthetic techniques to generate Nafion with controlled blockiness and the lack of tools appropriate to directly characterize the relationship between the transport properties and nanostructure at the atomistic level.

We report here the results of molecular dynamics (MD) simulations, which provide detailed information about how the dynamical and structural properties are coupled with each other. MD techniques are especially appropriate for PEMFC since we can use these techniques to discover the nanostructure for the hydrated Nafion without assuming a priori any specific model. Thus, by equilibrating thoroughly the initial structures used in the MD simulation, we may determine how the nanostructure depends on such variables as water content, temperature, and molecular architecture of the polymer. Many factors in the molecular architecture can be explored, but we focus herein on the monomeric sequence expressing how comonomers are statistically arranged along a chain. Nafion is a copolymer composed of polar and nonpolar monomeric units and is currently synthesized through the free radical polymerization.[43,44] As a result, the monomeric sequence is determined by the monomer reactivity ratio.[45] However, the specific monomeric sequence in Nafion chains has not been clearly characterized in experiments, and its effect on the nanostructure has not been investigated. Some previous modeling studies[25,46−50] have been reported but not on the nanostructure.

Our study uses full atomistic MD simulations to *predict* the nanostructure of hydrated Nafion 117 with a focus on investigating the effect of the monomeric sequence of polar (P) and nonpolar (N) monomeric units in Nafion on the nanophase-segregated morphology and the water/hydronium transport. We confine this study to the effect of monomer sequence on phase segregation and transport in the amorphous phase of hydrated Nafion. It has been suggested that Nafion membranes may have a small crystalline component[51] of 3−8 vol % in the unhydrolyzed polymer,[52] and it is suggested that this decreases with hydration.[53] However, no role of crystallinity in the transport properties in Nafion membranes has yet been demonstrated.

2. Simulation Details

All simulations were carried out using a fully atomistic model of Nafion 117, water, and hydronium. To assess the effect of monomeric sequence on the properties of interest, we prepared Nafion 117 chains (equivalent weight 1150 with $x = 7$, $y = 1$, $z = 1$, and $n = 10$ in Figure 1) with the two dramatically different monomeric sequences shown in Figure 2:

(1) Dispersed: Here the $(N_7P)_{10}$ sequence has the PSVE unit evenly spaced every 7 TFE units

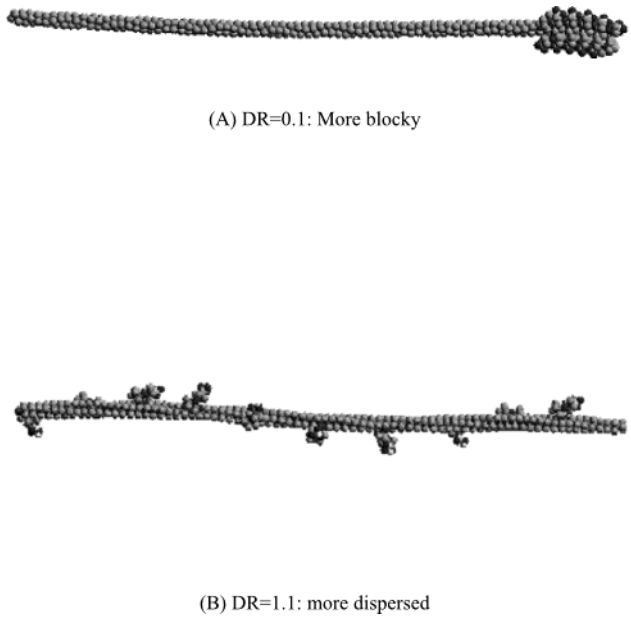

Figure 2. Two monomeric sequences of Nafion 117 studied here: (a) DR = 0.1 (more blocky) and (b) DR = 1.1 (more dispersed).

(2) Blocky: Here the polymer structure is a diblock copolymer with a $N_{70}P_{10}$ sequence in which all 10 PSVE units gather at the end of a chain of 70 TFE units.

We can distinguish these two cases by the degree of randomness (DR) defined as:

$$DR = \frac{1}{\bar{L}_A} + \frac{1}{\bar{L}_B} \tag{1}$$

where $\bar{L}_X$ is the average number of monomers of type X (X=A or B) that come together in a block. DR can range from 0.0 to 2.0. It is 0.0 for the homopolymer, 1.0 for the random copolymer, and 2.0 for an alternating copolymer,

Thus, DR decreases as the blockiness of the chain increases.[54] Thus

- DR = 1.1 for our *dispersed* case in which the ionizable monomeric unit is uniformly distributed along the chain. For the fully extended chain, the distance between adjacent sulfonate groups would be ∼22 Å.
- DR = 0.1 for the *blocky* case. For the fully extended chain, the distance between adjacent sulfonate groups would be ∼6 Å.

We realize that current synthetic techniques cannot achieve either of these monomeric sequences for Nafion 117. Probably current materials lead to DR somewhere between 0.1 and 1.1. Our goal here is to determine how the monomeric sequence affects the structural and dynamical characteristics of hydrated Nafion system as a prototype for developing new polyelectrolyte membranes. However, should we find that a particular sequence lead to particularly desirable properties, we are confident that synthetic chemists would find a way to achieve this structure.

We constructed the initial sample structures of hydrated Nafion using the Amorphous Builder of Cerius2,[55] which uses Monte Carlo techniques to build an amorphous structure with a three-dimensional periodic cell. However, as described below, we follow this Monte Carlo build with an extensive series of annealing simulations in which the volume and temperature are varied systematically to achieve a fully equilibrated system at the target temperature and pressure. We emphasize here that we have *not* biased the predicted structure by imposing any

particular geometry (cylinders, spheres, lamellae) for the distribution of water in the system, nor have we imposed any particular density or packing. Rather our strategy of temperature and pressure MD annealing is designed to obtain an equilibrated distribution of water in an equilibrated polymer system.

Each simulated system consists of four Nafion chains with identical monomeric sequences corresponding to DR = 0.1 or 1.1 and 560 water molecules and 40 hydronium molecules (total number of atoms in the system is 4568). This corresponds to 15 water molecules per each sulfonate group (~20 wt % water content), which is the concentration expected when operating the fuel cell in an atmosphere with ~60% humidity.

All data in this paper were obtained from two independent samples using different initial configurations to provide an idea of the uncertainties. We assumed here that all sulfonate groups are ionized, as expected from their pK_a. This is in accordance with the IR experimental observations.[53,56]

In addition to the simulation cell with 4568 atoms described above, we prepared independent simulation cells that are 8 times larger to determine how the finite size influences the nanostructure. However, the dynamic properties (e.g., diffusion) reported here are based on the smaller system.

The annealing procedure for constructing the amorphous structure is as follows. Since the experimental data indicates that the density is ~1.75 g/cm^3 at 300 K for the H form of Nafion 117 with the same water content (15 water molecules per sulfonate group),[57,58] we built the initial polymer structure using a supercell appropriate for a density of 1.8 g/cm^3. Here we used Monte Carlo techniques to first grow the polymer and then we added waters or hydronium ions into the larger voids. Then we relaxed these initial structures by applying the following annealing procedure. First, the structure was gradually expanded by 50% of its initial volume over a period of 50 ps while the temperature was simultaneously increased from 300 to 600 K. Next NVT MD simulations were performed at 600 K with the expanded volume for 50 ps. Next, the structure was compressed back to the initial volume over 50 ps while cooling the temperature down to the target temperature (T = 300 K). These steps were repeated five times. Then at the final target density (1.8 g/cm^3), we first carried out 100 ps of NVT MD (fixed volume and Nose-Hoover thermostat[59−62] at 300 K) which was followed with 200 ps NPT MD at 1 atm to fully equilibrate the density and structure at the target temperature (300 K). This led to a final density of 1.67 g/cm^3 for the blocky case and 1.60 g/cm^3 for the dispersed case. The annealing simulations were performed with LAMMPS (large-scale atomic/molecular massively parallel simulator) code from Plimpton at Sandia (modified to handle our force fields).[63,64] The equations of motion were integrated using the Verlet algorithm[65] with a time step of 1.0 fs, and the particle−particle particle−mesh (PPPM) method[66] was used for the electrostatic interactions.

After annealing the structures as described above, we performed MD simulations with the LAMMPS code at two temperatures, 300 and 353.15 K (the relevant temperatures for fuel cell operation) under NPT conditions for 3 ns for the 4568 atom systems and 200 ps for the 36 544 atom systems.

To describe inter- and intramolecular interactions, we used the DREIDING force field[67] (previously used by other investigators to study hydrated Nafion system[25,47,48,68]) but with the fluorocarbon parts described with a recently developed force field[69] and the water described using the F3C force field.[70] We used the standard combination rules of DREIDING in mixing

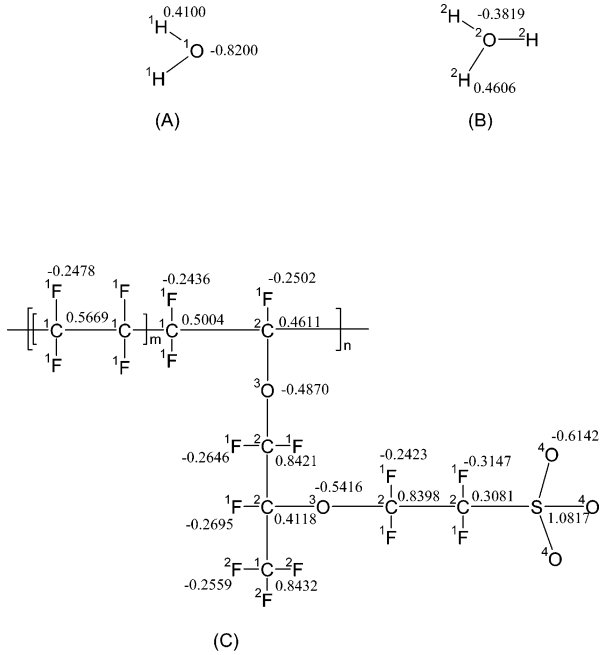

Figure 3. Chemical structure and partial charges of (A) water, (B) hydronium, and (C) ionized Nafion. The superscripts left and above atoms denote the atom types used in Table 1.

these FF. The total potential energy is given as follows:

$$E_{total} = E_{vdW} + E_Q + E_{bond} + E_{angle} + E_{torsion} \qquad (2)$$

where E_{total}, E_{vdW}, E_Q, E_{bond}, E_{angle}, and $E_{torsion}$ are the total energies and the van der Waals, electrostatic, bond stretching, angle bending, and torsion components, respectively. The specific force field atoms types on each atom are shown in Figure 3 and listed in Table 1.

3. Results and Discussion

3.1. Nanophase-Segregated Structure. We observed water−polymer segregation for both monomer sequences as shown in Figure 4. The calculated densities (ρ) of the equilibrated systems are

- At 300 K: $\rho = 1.67 \pm 0.01$ g/cm^3 for DR = 0.1 and 1.60 ± 0.01 g/cm^3 for DR = 1.1
- At 353.15 K: $\rho = 1.62 \pm 0.02$ g/cm^3 for DR = 0.1, and 1.55 ± 0.03 g/cm^3 for DR = 1.1

Thus, the dispersed system is predicted to have a density 4% smaller than the blocky system. The simulations for the blocky system leads to a density 5% smaller than the experimental value (~1.75 g/cm^3 at 300 K) for the H form of Nafion 117 with the same water content (15 water molecules per sulfonate group).[57,58] A part of the explanation for our calculated density being smaller than experiment could be because our simulations considered purely amorphous systems, whereas the experimental systems are thought to have ~3−8% crystallinity.[52,71−73]

We find that all sulfonate groups are in the water phase, which is consistent with the experimental observation of complete dissociation of the sulfonate groups in hydrated Nafion.[53,56] For both sequences, we find that 20 wt % water content (λ = 15 water per sulfonate), leads to a percolated nanophase structure for the hydrophilic domain.

These two monomeric sequences (DR = 0.1 vs DR = 1.1) lead to a noticeable difference in the nanophase-segregated structure (see Figure 4). The sulfonate groups in the *blocky polymer* aggregate themselves to form a cluster-like morphology

TABLE 1: Force Field Used for the Hydrated Nafion System

$$E_{\mathrm{vdW}}(R) = D_0\left\{\left(\frac{R_0}{R}\right)^{12} - 2\left(\frac{R_0}{R}\right)^{6}\right\},\ E_Q{}^a = 322.0637\sum_{i>j}\frac{Q_iQ_j}{\epsilon R_{ij}}$$

$$E_{\mathrm{bond}}(R) = \frac{1}{2}K_b(R - R_0)^2,\ E_{\mathrm{angle}}(\theta) = \frac{1}{2}K_\theta(\theta - \theta_0)^2$$

$$E_{\mathrm{torsion}}(\phi) = \sum_n \frac{1}{2}V_n[1 - d_n\cos(n\phi)]$$

E_{vdW}	^{1}H(HF3C), ^{2}H(HH3O)	$R_0{}^c$	0.9000	$D_0{}^d$	0.0100
	^{1}O(OF3C), ^{2}O(OH3O)	R_0	3.5532	D_0	0.1848
	^{1}C(C_3T)^b	R_0	3.8837	D_0	0.0844
	^{2}C(C_3)	R_0	3.8983	D_0	0.0951
	^{1}F(F_), ^{2}F(F_3)^b	R_0	3.3953	D_0	0.0496
	^{3}H(H_A)	R_0	3.1950	D_0	0.0001
	^{3}O(O_3), ^{4}O(O_2),	R_0	3.4046	D_0	0.0957
	S(S_3)	R_0	4.0300	D_0	0.3440
E_{bond}	OF3C − HF3C	R_0	1.0000	$K_b{}^e$	500.0000
	OH3O − HH3O	R_0	0.9820	K_b	1085.9565
	C_3T − C_3T	R_0	1.4982	K_b	429.3204
	C_3 − C_3	R_0	1.5300	K_b	700.0000
	C_3T − C_3	R_0	1.5300	K_b	700.0000
	C_3 − O_3	R_0	1.4200	K_b	700.0000
	C_3(T) − F_(3)	R_0	1.3360	K_b	605.2595
	C_3 − S_3	R_0	1.8000	K_b	700.0000
	S_3 − O_3	R_0	1.6900	K_b	700.0000
	S_3 − O_2	R_0	1.4800	K_b	700.0000
	O_3 − H_A	R_0	0.9800	K_b	700.0000
E_{angle}	HF3C−OF3C−HF3C	$\theta_0{}^f$	109.4700	$K_{\theta g}$	120.0000
	HH3O−OH3O−HH3O	θ_0	113.4000	K_θ	79.0263
	X − C_3(T)−X	θ_0	109.4710	K_θ	100.0000
	C_3(T)−C_3(T)−C_3(T)	θ_0	122.5536	K_θ	106.2739
	C_3(T)−C_3(T)−F_(3)	θ_0	118.3191	K_θ	100.3366
	F_(3) − C_3(T) −F_(3)	θ_0	121.5020	K_θ	108.2396
	X − S_3 −X	θ_0	109.4710	K_θ	350.0000
	O2 − S_3 − O2	θ_0	115.5000	K_θ	350.0000
E_{torsion}	X − C_3(T) −C_3(T) − X	V_3 (d_3)^h	2.0000 (−1)		
	C_3T-C_3T −C_3T − C_3T	V_3 (d_3)	6.4342 (1)		
	F_(3)-C_3T −C_3T − C_3T	V_3 (d_3)	8.2444 (1)		
	F_(3)-C_3T−C_3T − F_(3)	V_3 (d_3)	8.0848 (−1)		
	X − C_3(T) − O_3 − X	V_3 (d_3)	2.0000 (−1)		
	X − C_3(T) − S_3 − X	V_3 (d_3)	2.0000 (−1)		
	X − S_3(T) − O_3 − X	V_2 (d_2)	2.0000 (−1)		

[a] Q_i and Q_j are atomic charge of atom i and j, respectively. Except for water all atomic charges were calculated from QM Mulliken populations at the level of 6-31G**/B3LYP. The atomic charge for water molecules are from the F3C model in ref 70. [b] The original van der Waals parameters were refitted to the Lennard-Jones 12−6 potential. function. [c] Å for R_0. [d] kcal/mol for D_0. [e] kcal/mol/Å^2 for K_b [f] Degree for θ_0 [g] kcal/mol/degree^2 for K_θ [h] kcal/mol for V_n.

of the hydrophilic phase with water as suggested by Hsu and Gierke.[11,12] However, the hydrophilic phase does *not* have the spherical shape they suggested. In contrast, we find that the *dispersed sequence* leads to a somewhat uniform distribution of sulfonate group throughout the system and does not exhibit phase segregation to the extent observed for the blocky case.

Another structural difference is found in the pair correlation functions for sulfur−sulfur pairs, $g_{S-S}(r)$ (shown in Figure 5 for 353.15 K). This pair correlation function indicates the probability of finding two S atoms at a distance r, averaged over the equilibrium trajectory as in eq 3

$$g_{A-B}(r) = \left(\frac{n_B}{4\pi r^2 dr}\right)\Big/\left(\frac{N_B}{V}\right) \tag{3}$$

where n_B is the number of particle B located at the distance r in a shell of thickness dr from particle A, N_B is the number of B particles in the system, and V is the total volume of the system. Although the S−S distances for the extended polymer chains would be quite different (∼ 22 for dispersed and ∼ 6 Å for blocky), Figure 5 shows clearly that the S−S distance for the dispersed system of 6.8 Å is comparable with the 6.0 Å S−S distance for the blocky system. Thus, the equilibrated Nafion chains fold to render comparable S−S distances independent of sequence. Even so, the blocky case still has more S−S closer neighbors than the dispersed case.

Figure 5 also displays the intrachain contribution to $g_{S-S}(r)$ along individual chains. This shows that for the blocky structure

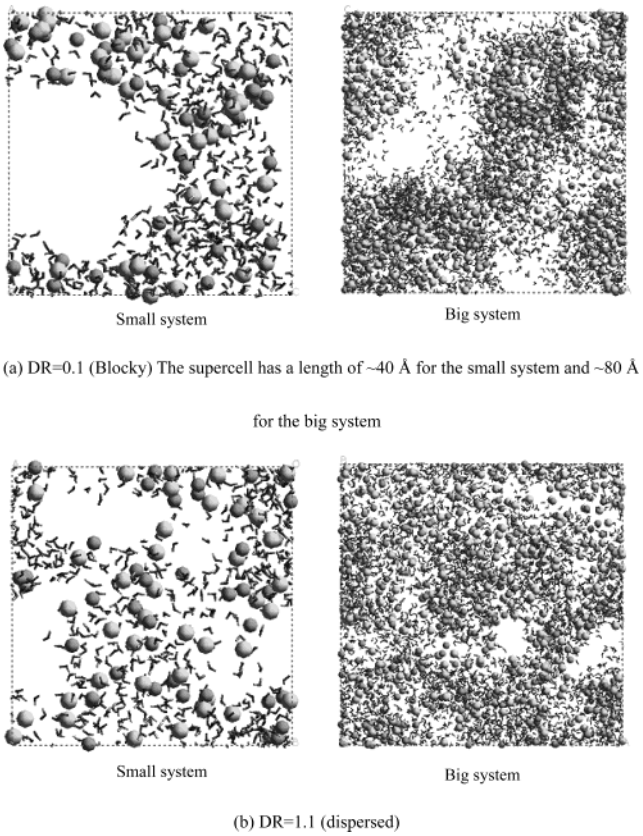

Figure 4. Nanophase-segregated structures of hydrated Nafion predicted from the simulations at 353.15 K. Nafion backbone atoms have been deleted from the pictures; hence the white regions are the parts occupied by the Nafion backbone. Bright gray spheres represent sulfur atoms and dark gray spheres represent the oxygen atoms in hydronium molecules: (a) DR = 0.1 (blocky) and (b) DR = 1.1 (dispersed).

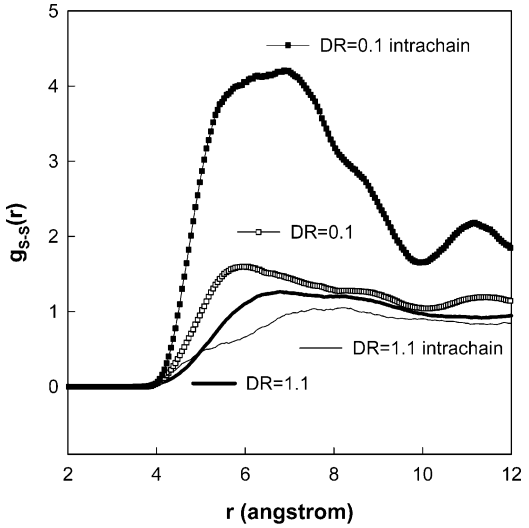

Figure 5. Sulfur−sulfur pair correlation function, $g_{S-S}(r)$ for hydrated Nafion 117 with 20 wt % of water (λ = 15) at 353.15 K for the blocky sequence (DR = 0.1) and the dispersed sequence (DR = 1.1) of the polar/nonpolar monomers.

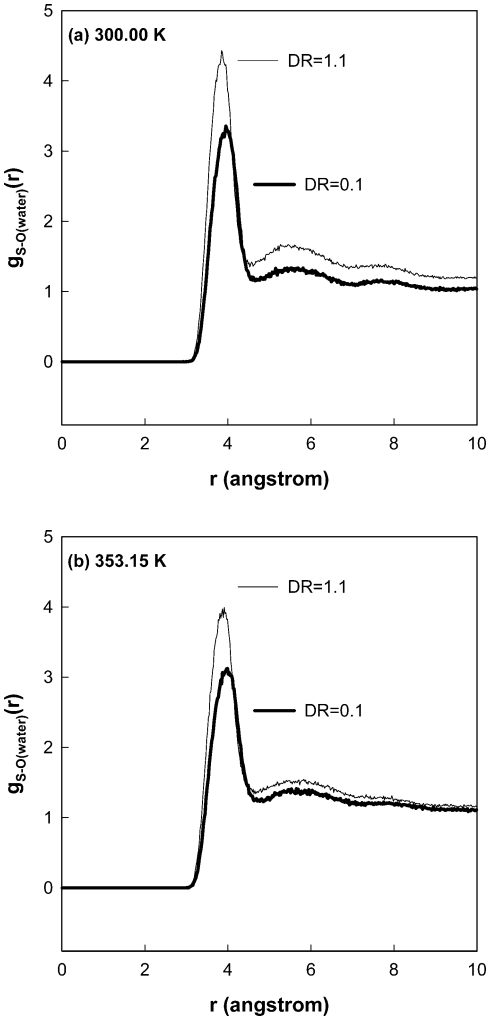

Figure 6. Sulfur−oxygen (water) pair correlation function, $g_{S-O(water)}(r)$ for hydrated Nafion 117 with 20 wt % of water ($\lambda = 15$) for two sequences of polar/nonpolar monomers: DR = 0.1 (blocky) and DR = 1.1 (dispersed). (a) 300 and (b) 353.15 K.

the dominant contribution at short distances to $g_{S-S}(r)$ comes from sulfonates in the *same* chain while for the dispersed system, the interchain contributions are significant.

Figure 6 shows the pair correlation functions of sulfur with the water oxygens, $g_{S-O(water)}(r)$. This indicates that the first water solvation shell of the sulfonate group has larger intensity and closer distances for the dispersed case than for the blocky case. This is reflected in the water coordination number for sulfonate group calculated from the first solvation shell:

- At 300 K, the water coordination number is 5.66 for the DR = 1.1 and 5.36 for the DR = 0.1,
- At 353.15 K, the water coordination number is 5.59 for the DR = 1.1 and 5.35 for the DR = 0.1.

This means that the sulfonate groups in the dispersed case are more solvated by water than in the blocky case and that the water molecules in the first shell are bound to the sulfonate groups more strongly for the dispersed than for blocky case.

To evaluate quantitatively the extent of phase segregation in the system, we calculated the structure factor, $S(q)$ as obtained in small angle scattering experiments (SAXS and SANS). using the following equation:

$$\mathbf{S(q)} = \langle \sum_{r_i} \sum_{r_j} \exp(i\mathbf{q}\cdot\mathbf{r}_{ij})(\xi^i\xi^j - \langle\xi\rangle^2)\rangle/L^3 \qquad (4)$$

where the angular bracket denotes a thermal statistical average, ξ^i represents a local density contrast, $(\phi^j_A - \phi^j_B)$, and $\boldsymbol{q}$ and $\mathbf{r}_{ij}$ are the scattering vector and the vector between the sites i and j, respectively. Previous simulations using periodic boundary conditions have also investigate the phase-segregated structure in copolymer systems[74−79] and polymer blend systems[80−90] by calculating the structure factor.

Analysis of SAXS experiments uses the electron density contrast and SANS experiments use deuterium density contrast. For our analysis we assigned an artificial density contrast as follows. The local density variable ϕ^j_A is equal to 1 if the site j is occupied by a hydrophilic entity such as water or hydronium and equal to 0 otherwise, and ϕ^j_B is equal to 1 if the site is occupied by hydrophobic entities such as Nafion and equal to 0 otherwise.

The quantity $\mathbf{S(q)}$ is spherically averaged as follows:

$$S(q) = \sum_{|\mathbf{q}|} \mathbf{S(q)} / \sum_{|\mathbf{q}|} 1 \qquad (5)$$

with $q = (2\pi/L)n$, where $n = 1, 2, 3, \ldots$ denotes that, for a given n, a spherical shell is taken as $n - 1/2 \le qL/2\pi \le n + 1/2$. The structure factor profiles in Figure 7 were obtained as a function of scattering vector, $\mathbf{q}$. We found that these structure profiles were almost completely established during the annealing procedure and did not change significantly during the subsequent equilibrium MD simulations (3 ns for the small system and 200 ps for the big system). This is because the glassy structures of the membranes are not able to undergo a significant reorganization within the time scale of our simulations. We see that for low q, the intensity of $S(q)$ for the blocky Nafion (DR = 0.1) is stronger than the DR = 1.1 independent of the system, which means that the blocky Nafion has a better developed phase-segregated structure. A similar observation based on SAXS was reported by the Kreuer and Maier, who found that the more phase-segregated Nafion has stronger intensity at low q than the less phase-segregated sulfonated poly (ether ether ketone) (PEEK).[18,91]

Experimental SAXS and SANS,[12,15,20] studies of Nafion 117 reported that the typical ionomer peak is at $q = \sim 0.13$ Å^{-1} as shown by the dashed line in Figure 7. This corresponds to a characteristic segregation distance of ∼ 50 Å. For the small system, the differences observed in the profile (Figure 7a) in the range of $q < 0.15$ are caused by repetitive self-images of the morphology through imposition of periodic boundary conditions. That is, the finite-size of the small system unit cell dimensions (∼40 Å) restricts the structural development beyond the size of the simulation cell. In contrast, the big system (cell dimensions ∼80 Å) leads to a phase-segregated structure for the blocky case that has a peak at $q = 0.13$ Å^{-1} leading to a characteristic segregation distance ∼50 Å. This is comparable to the experiment which finds the same characteristic distance for 18.5% water.[11] In contrast for the large unit cell, the dispersed sequence leads to a more dispersed profile with $q \sim 0.20$ Å^{-1} corresponding to a characteristic segregation distance of ∼30 Å, which is smaller than the experimental value. These results suggest that the blockiness of Nafion in the experimental system is intermediate between these two cases but closer to the blocky case.

Starkweather[71] studied Nafion with minimal water content and found that the crystallite size is ∼44 Å, suggesting that 34 carbon atoms line up along the c axis. This would imply that the monomeric sequence corresponds to $(N_{14}P_2)_n$ statistically, giving DR=0.57, which is intermediate between our two cases.

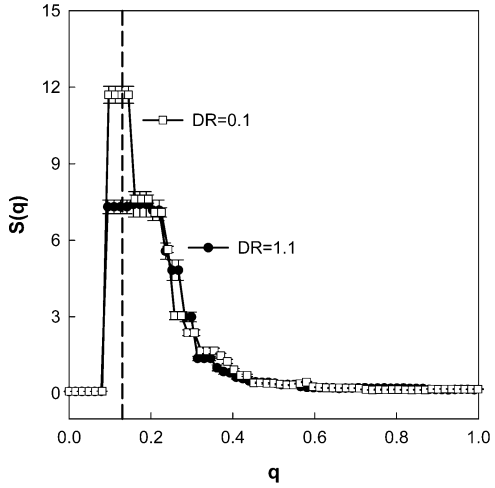

(a) Small system

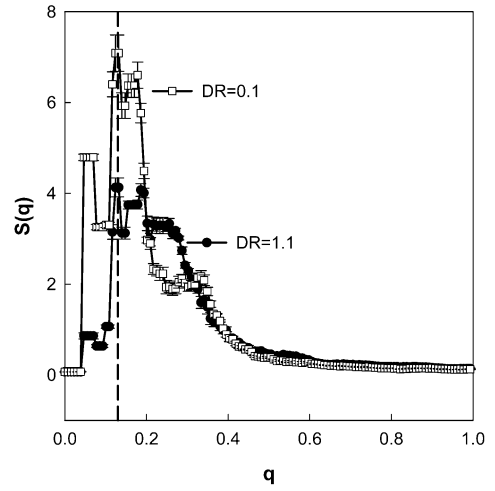

(b) Big system

Figure 7. Structure factor profile for hydrated Nafion with 20 wt % of water content ($\lambda = 15$) simulated at 353.15 K. The dashed lines indicate the location of the typical ionomer peak of Nafion 117 observed in experiments at $q = 0.13$ Å^{-1}.

3.2. Heterogeneity of the Water−Nafion Interface. In this paper, we use the terminology "heterogeneity of interface" to expresses how differently the sulfonate groups are arranged at the interface due to the difference in monomeric sequence. Previous theoretical studies have mentioned that the distribution of sulfonate groups in the nanophase-segregated or nanopore structure in hydrated Nafion membrane could affect the transport phenomena, but the only explicit model has been to assume a uniform distribution of fixed sulfonate groups in cylindrical geometry.[40−42,46,92] In contrast, we predicted the distribution of sulfonate groups by using a combination of Monte Carlo building and the MD annealing and equilibration without any assumptions about the distribution.

Our initial conjecture was that the changes in blockiness in monomeric sequence might lead to a different extent of segregation at the interface in addition to a modified phase-segregation for the whole system (Figure 8). To investigate this, we analyzed the interface by the following procedure.

First, we defined the interface between hydrophilic water phase and hydrophobic polymer phase as the Connolly van der Waals surface of the water phase.

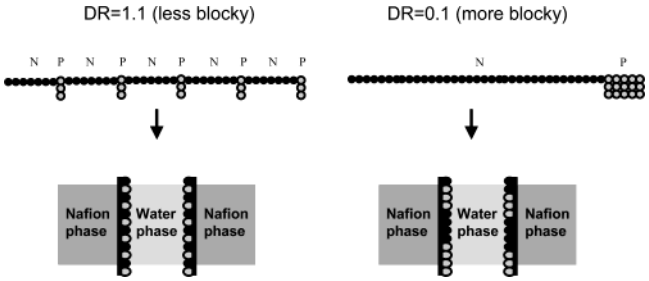

Figure 8. Schematic representation of the heterogeneity of the interface between hydrophilic water phase and hydrophobic Nafion phase caused by the different monomeric sequences.

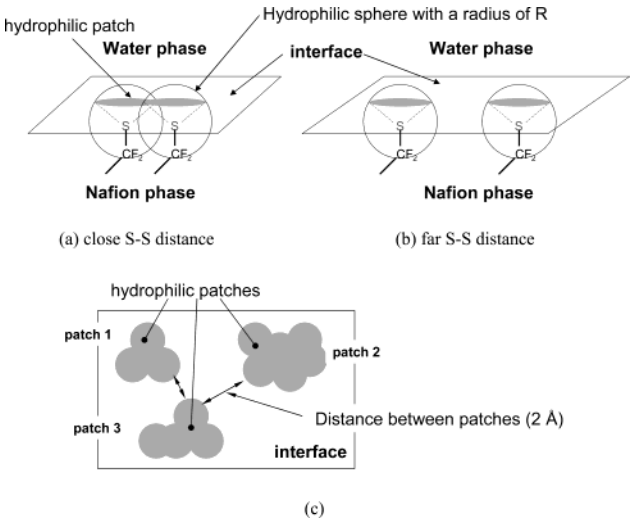

Figure 9. Definition of the hydrophilic sphere and interface.

Second, we introduced a hydrophilic sphere centered on each sulfur atom with a radius of R (Figure 9a,b). The space inside this sphere is assumed to be influenced by the existence of the sulfonate group.

Third, the overlapped cross section of this hydrophilic sphere with the interface is counted as part of the *hydrophilic patch* (Figure 9a,b). The rest of the interface is considered as the *hydrophobic interface* in which the water molecules contact the hydrophobic polymer phase. We consider these hydrophilic patches to be connected if they are within water diameter distance.

Figure 9a,b presents two cases differing by the relative distance between sulfonate groups. Figure 9a displays a closer distance than Figure 9b. As a result, the former has more overlap between the hydrophilic interfaces, thereby forming a single large hydrophilic patch whereas the latter has two small patches. As a result, the total area of the hydrophilic patch is smaller for the former than for the latter. Figure 9c shows a schematic example of the interface in which three hydrophilic patches are separated from each other. Here, to identify individual patches, we selected (arbitrarily) 2 Å as the distance between patch boundaries.

By applying these concepts, we decomposed the interface between the water phase and the Nafion phase into hydrophilic and hydrophobic patches as shown in Figure 10. Although it would seem that the hydrophilic patches would be well defined near by each sulfonate group, the quantitative difference between the DR = 1.1 and the DR = 0.1 is not sufficiently different to be clear in this visual comparison. To quantify the difference, we calculated the fraction of the hydrophilic patch area with respect to the whole interfacial area as a function of radius of hydrophilic sphere as in Figure 11. For a small radius (<4 Å),

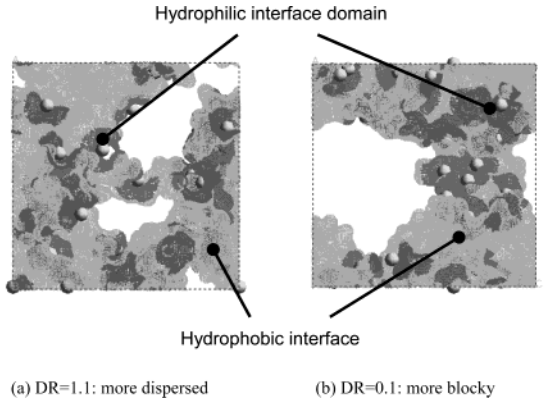

Figure 10. Decomposition of the interface into the hydrophilic and the hydrophobic portions.

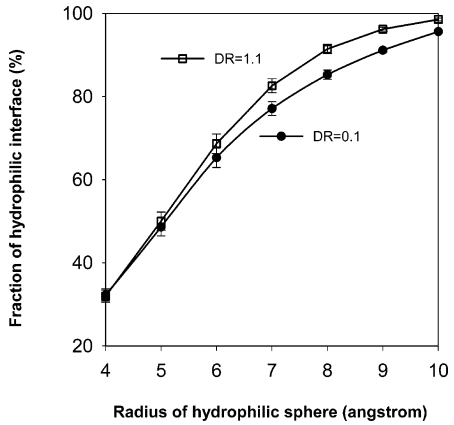

Figure 11. Fraction of the hydrophilic patch as a function of the radius for the hydrophilic sphere.

the fraction of hydrophilic area is nearly the same (~32%) for both monomeric sequences because the hydrophilic spheres overlap little, whereas for large values of the radius R (>10 Å), the entire interface is engulfed by the hydrophilic spheres so that the area fractions for both cases become similar again. In the intermediate range (4 Å < R < 10 Å), the difference in the spatial distribution of the hydrophilic spheres between the blocky (DR = 0.1) and the dispersed (DR = 1.1) cases becomes evident: the dispersed case produces a more dispersed distribution of the sulfonate groups on the interface and the fraction increases faster with the radius compared with the segregated interface in the blocky case. However, even for R = 4 Å where the fractions of hydrophilic patch are almost the same for the DR = 0.1 and the DR = 1.1, the *size distributions* of hydrophilic patchs are remarkably different as shown in Figure 12. There we see that the blocky case has a larger population of large patches than the dispersed case. This indicates that the hydrophilic patches at the interface are more segregated in the blocky case than in the dispersed case.

Summarizing, all of the above analyses indicate that the blocky (DR = 0.1) case has a more segregated interface between the water and polymer phase than does the dispersed case (DR = 1.1).

3.3. Transport of Water and Hydronium. It is reasonable to expect that the transport properties of water and hydronium depend on the heterogeneous nanophase-segregated structures, which in turn are coupled with the monomeric sequence. As mentioned in previous sections, experimental studies[18,39,91] on the transport in nanostructures with varying extents of phase segregation observe that the diffusion of water and protons is enhanced in Nafion over sulfonated PEEK because of the wider

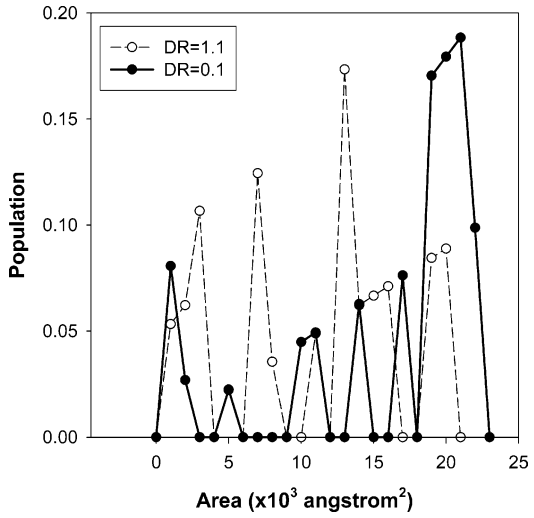

Figure 12. Size distribution of the hydrophilic patch for the small system simulated at 353.15 K.

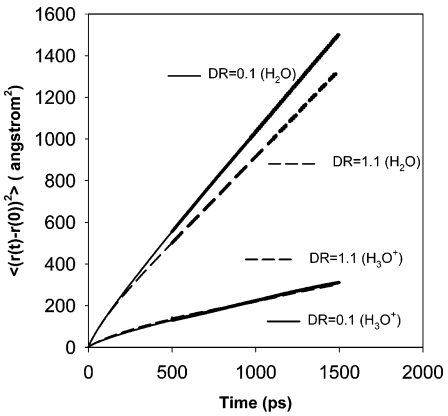

Figure 13. Mean square displacement as a function of time of water and hydronium in the hydrated Nafion system simulated at 353.15 K.

water channels in Nafion. Figure 13 shows the mean square displacement (MSD) of water and hydronium calculated from the 3 ns trajectories. As expected, there is greater water molecule diffusion in the more segregated structure. This is quite consistent with experimental results.[18,39,91]

In contrast, we find that the diffusion of hydronium molecules is rather insensitive to the monomer sequence. This would seem to disagree with the experimental observation reporting that proton diffusion is also enhanced in relatively larger-scale phase-segregated structures.[18,39,91] However, our current classical MD simulations describe only the *vehicular motion* of hydronium. That is, our calculations distinguish H_3O^+ from H_2O so that proton diffusion is the same as hydronium diffusion and does *not* include the contributions from protons hopping from one H_2O to another. We expect that the difference in proton diffusion measured experimentally is mainly due to differences in proton hopping (which might be strongly affected by the interface distribution of sulfonates).

Using $\langle (r(t) - r(0))^2 \rangle = 6Dt$ with the linear part of MSD in Figure 13, we calculate the diffusion coefficients for water and hydronium listed in Table 2. The calculated diffusion coefficients of water at 300.00 K are $(0.591 \pm 0.035) \times 10^{-5}$ cm^2/s for DR = 0.1 and $(0.458 \pm 0.043) \times 10^{-5}$ cm^2/s for DR = 1.1 and, at 353.15 K, are $(1.618 \pm 0.050) \times 10^{-5}$ cm^2/s for DR = 0.1 and $(1.431 \pm 0.065) \times 10^{-5}$ cm^2/s for DR = 1.1.

TABLE 2: Diffusion Coefficients and Estimated Activation Energy for Water and Hydronium Predicted from the MD Simulations

	water			hydronium (H_3O^+)		
	D ($\times 10^{-5}$ cm^2/s)			D ($\times 10^{-5}$ cm^2/s)		
	300.00 K	353.15 K	E_a (kJ/mol)	300.00 K	353.15 K	E_a (kJ/mol)
DR = 0.1	0.591 ± 0.035	1.618 ± 0.050	16.68	0.158 ± 0.008	0.294 ± 0.044	10.32
DR = 1.1	0.458 ± 0.043	1.431 ± 0.065	18.87	0.115 ± 0.010	0.290 ± 0.062	10.32

These values can be compared the experimental values[93] (for a similar water content of 14 water molecules per sulfonate group) 0.5 $\times$ 10^{-5} cm^2/s at 298.15 K and 1.25 $\times$ 10^{-5} cm^2/s 353.15 K.

Based on the temperature dependence, we calculate an activation energy of 16.68 kJ/mol for the DR = 0.1 case and 18.87 kJ/mol the DR = 1.1 case,

This is comparable with the experimental values (11.6∼20.08 kJ/mol),[4,93] We consider that the consistent agreement with experiment supports the validity of our simulations as a model for real Nafion.

These dynamical simulations confirm the results from analyzing the equilibrium structures that water molecules in the more phase-segregated structure of the blocky system diffuse more rapidly than in the less segregated dispersed. This is consistent with experimental observations.[18,39,91] As shown in Table 2, the calculated vehicular diffusion coefficients of hydronium molecules at 300 K are (0.158 ± 0.008) $\times$ 10^{-5} cm^2/s for DR = 0.1 and (0.115 ± 0.010) $\times$ 10^{-5} cm^2/s for DR=1.1 and, at 353.15 K, are (0.294 ± 0.044) $\times$ 10^{-5} cm^2/s for DR = 0.1 and (0.290 ± 0.062) $\times$ 10^{-5} cm^2/s for DR = 1.1.

These values are also comparable with the experimental values (0.7 $\times$ 10^{-5} at 303.15 K and 1.0 $\times$ 10^{-5} cm^2/s at 353.15 K).[94,95] Our observation that the vehicular contribution to proton conductivity is not sensitive to the difference in nanophase segregation with 20 wt % water content, suggests that there may be a compensation of the effect of a more segregated structure (favorable for transport in the hydrophilic phase) and the heterogeneous distribution of ionic groups in the interface (that may decrease ionic mobility through an increase in the ionic condensation).

4. Conclusions

Using atomistic MD simulations, we investigated the effect of monomeric sequence of Nafion chain on the nanophase-segregation and transport in hydrated Nafion systems with 20 wt % of water content (15 water molecules per sulfonate group) at 300 and 353.15 K.

For both monomeric sequences (the blocky DR = 0.1 case and the dispersed DR = 1.1 case) simulating Nafion, we find clearly segregated structures with well-defined water and polymer phases. However, the pair correlation function for sulfur−sulfur pairs and for sulfur−oxygen (water) pairs indicate that the sulfonate groups in the dispersed case are slightly more dispersed and slightly more solvated by water than in the blocky case.

The calculated structure factor shows that the monomer sequence of the polyelectrolyte has a noticeable effect on the extent of phase-segregation: the blocky sequence has better phase segregation than the dispersed case. The characteristic dimension of the simulated hydrophilic clusters is ∼50 Å for the blocky case (DR = 0.1) and ∼20−30 Å for the dispersed case (DR = 1.1) in good agreement with the 40−50 Å from small-angle scattering experimental observations. This comparison suggests that real Nafion is intermediate but closer to the blocky case.

The interface between the water and polymer phases was analyzed to determine how sulfonate groups are arranged at the interface. We found that the interface has a heterogeneous structure, consisting of hydrophobic and hydrophilic patches. The segregation of the ionic groups in the linear polymer chain (blocky) produces a better segregation of these hydrophobic and hydrophilic patches in the water-polymer interface. The degree of segregation and size of the patches is larger in the blocky sequence than the dispersed one.

Water transport in these systems is shown to depend on these structural differences caused by the monomeric sequence: the water molecules with the blocky sequence leading to larger diffusion than for the dispersed sequence, because the blocky case leads to larger clusters and channels than the latter. This result is consistent with the experimental studies on the difference between Nafion and sulfonated PEEK. In contrast, we do *not* find a significant difference in hydronium vehicular diffusion. Thus, we conclude that the proton hopping mechanism (not vehicular contributions) must be responsible for the experimentally observed differences in proton diffusion.

Acknowledgment. This research was supported in part by General Motors (GAPC, Dr. G. Voecks). The facilities of the Materials and Process Simulation Center used for these studies are supported by DURIP-ARO, DURIP-ONR, IBM-SUR, and NSF (MRI) and other support for the MSC comes from MURI-ARO, MURI-ONR, DOE, ONR, NSF-CSEM, NIH, General Motors, ChevronTexaco, Seiko-Epson, Beckman Institute, and Asahi Kasei.

References and Notes

(1) Carrette, L.; Friedrich, K. A.; Stimming, U. *ChemPhysChem* **2000**, *1*, 162.
(2) Eisenberg, A., Yeager, H. L., Eds.; *Perfluorinated Ionomer Membranes*; American Chemical Society: Washington, DC, 1982.
(3) Yeager, H. L.; Steck, A. *Anal. Chem.* **1979**, *51*, 862.
(4) Yeo, S. C.; Eisenberg, A. *J. Appl. Polym. Sci.* **1977**, *21*, 875.
(5) Eisenberg, A.; King, M. In *Polymer Physics*; Stein, R. S., Ed.; Academic Press: New York, 1977.
(6) Scibona, G.; Fabiani, C.; Scuppa, B. *J. Membr. Sci.* **1983**, *16*, 37.
(7) Eisenberg, A. *Macromolecules* **1970**, *3*, 147.
(8) Falk, M. *Can. J. Chem.* **1980**, *58*, 1495.
(9) Duplessix, R.; Escoubes, M.; Rodmacq, B.; Volino, F.; Roche, E.; Eisenberg, A.; Peneri, M. In *Water in Polymer*; American Chemical Soceity: Washington, DC, 1980.
(10) Rodmacq, B.; Coey, J. M.; Escoubes, M.; Roche, E.; Duplessix, R.; Eisenberg, A.; Pineri, M. In *Water in Polymers*; Rowland, S. P., Ed.; American Chemical Soceity: Washington, DC, 1980.
(11) Gierke, T. D.; Munn, G. E.; Wilson, F. C. *J. Polym. Sci.: Polym. Phys. Ed.* **1981**, *19*, 1687.
(12) Hsu, W. Y.; Gierke, T. D. *J. Membr. Sci.* **1983**, *13*, 307.
(13) Yeager, H. L.; Steck, A. *J. Electrochem. Soc.* **1981**, *128*, 1880.
(14) Verbrugge, M. W.; Hill, R. F. *J. Electrochem. Soc.* **1990**, *137*, 886.
(15) Gebel, G. *Polymer* **2000**, *41*, 5829.
(16) James, P. J.; Elliott, J. A.; McMaster, T. J.; Miles, J. M. *J. Mater. Sci.* **2000**, *35*, 5111.
(17) James, P. J.; McMaster, T. J.; Newton, J. M.; Miles, M. J. *Polymer* **2000**, *41*, 4223.
(18) Kreuer, K. D. *J. Membr. Sci.* **2001**, *185*, 29.
(19) Haubold, H.-G.; Vad, T.; Jungbluth, H.; Hiller, P. *Electrochim. Acta* **2001**, *46*, 1559.
(20) Rollet, A.-L.; Gebel, G.; Simonin, J.-P.; Turq, P. *J. Polym. Sci.: Part B: Polym. Phys.* **2001**, *39*, 548.

(21) Rollet, A.-L.; Diat, O.; Gebel, G. *J. Phys. Chem. B* **2002**, *106*, 3033.
(22) Young, S. K.; Trevino, S. F.; Tan, N. C. B. *J. Polym. Sci.: Part B: Polym. Phys.* **2002**, *40*, 387.
(23) Tovbin, Y. K.; D'yakov, Y. A.; Vasutkin, N. F. *Russ. J. Phys. Chem.* **1993**, *67*, 2122.
(24) D'yakov, Y. A.; Tovbin, Y. K. *Russ. Chem. Bull.* **1995**, *44*, 1233.
(25) Vishnyakov, A.; Neimark, A. V. *J. Phys. Chem. B* **2001**, *105*, 7830.
(26) Mauritz, K. A.; Hora, C. J.; Hopfinger, A. J. In *Ions in Polymers*; Eisenberg, A., Ed.; American Chemical Society: Washington, DC, 1980.
(27) Datye, V. K.; Taylor, P. L.; Hopfinger, A. J. *Macromolecules* **1984**, *17*, 1704.
(28) Mauritz, K. A.; Rogers, C. E. *Macromolecules* **1985**, *18*, 483.
(29) Dreyfus, B. *Macromolecules* **1985**, *18*, 284.
(30) Eikerling, M.; Kornyshev, A. A.; Stimming, U. *J. Phys. Chem. B* **1997**, *101*, 10807.
(31) Tovbin, Y. K. *Russ. J. Phys. Chem.* **1968**, *72*, 55.
(32) Tovbin, Y. K.; Vasyatkin, N. F. *Colloid Surf. A* **1999**, *158*, 385.
(33) Verbrugge, M. W.; Hill, R. F. *J. Electrochem. Soc.* **1990**, *137*, 3770.
(34) Verbrugge, M. W.; Hill, R. F. *J. Electrochem. Soc.* **1990**, *137*, 893.
(35) Verbrugge, M. W.; Hill, R. F. *J. Electrochem. Soc.* **1990**, *137*, 1131.
(36) Zawodzinski, T. A.; Neeman, M.; Sillerud, L. O.; Gottesfeld, S. *J. Phys. Chem.* **1991**, *95*, 6040.
(37) Zawodzinski, T. A.; Derouin, C.; Radzinski, S.; Sherman, R. J.; Smith, V. T.; Springer, T. E.; Gottesfeld, S. *J. Electrochem. Soc.* **1993**, *140*, 1041.
(38) Zawodzinski, T. A.; Springer, T. E.; Davey, J.; Jestel, R.; Lopez, C.; Valerio, J.; Gottesfeld, S. *J. Electrochem. Soc.* **1993**, *140*, 1981.
(39) Kreuer, K. D. *Solid-State Ionics* **2000**, *136*−*137*, 149.
(40) Paddison, S. J.; Paul, R.; Zawodzinski, T. A. *J. Electrochem. Soc.* **2000**, *147*, 617.
(41) Paddison, S. J.; Paul, R.; T. A. Zawodzinski, J. *J. Chem. Phys.* **2001**, *115*, 7753.
(42) Paul, R.; Paddison, S. J. *J. Chem. Phys.* **2001**, *115*, 7762.
(43) Carlson, D. P. U.S. Patent No. 3,528,954, Du Pont, 1970.
(44) Kirsh, Y. E.; Smirnov, S. A.; popkov, Y. M.; Timashev, S. F. *Russ. Chem. Rev.* **1990**, *59*, 560.
(45) Odian, G. *Principles of Polymerization*; John Wiley & Sons: New York, 1991.
(46) Din, X.-D.; Michaelides, E. E. *AIChE J.* **1998**, *44*, 35.
(47) Elliott, J. A.; Hanna, S.; Elliott, A. M. S.; Cooley, G. E. *Phys. Chem. Chem. Phys.* **1999**, *1*, 4855.
(48) Vishnyakov, A.; Neimark, A. V. *J. Phys. Chem. B* **2000**, *104*, 4471.
(49) Vishnyakov, A.; Neimark, A. V. *J. Phys. Chem. B* **2001**, *105*, 9586.
(50) Jinnouchi, R.; Okazaki, K. *J. Electrochem. Soc.* **2003**, *150*, E66.
(51) Moore, R. B.; Martin, C. R. *Macromolecules* **1988**, *21*, 1334−1339.
(52) Timashev, S. F. *Physical chemistry of membrane processes*; Ellis Horwood: New York, 1991.
(53) Laporta, M.; Pegoraro, M.; Zanderighi, L. *Phys. Chem. Chem. Phys.* **1999**, *1*, 4619.
(54) Koenig, J. L. *Chemical Microstructre of Polymer Chains*; John Wiley & Sons: New York, 1980.
(55) *Cerius2 Modeling Environment, Release 4.0*; Accelrys Inc.: San Diego, CA, 1999.
(56) Gruger, A.; Regis, A.; Schmatko, T.; Colomban, P. *Vibr. Spectrosc.* **2001**, *26*, 215.
(57) Takamatsu, T.; Eisenberg, A. *J. Appl. Polym. Sci.* **1979**, *24*, 2221.
(58) Morris, D. R.; Sun, X. *J. Appl. Polym. Sci.* **1993**, *50*, 1445.
(59) Nose, S.; Klein, M. L. *J. Chem. Phys.* **1983**, *78*, 6928−6939.
(60) Nose, S. *J. Chem. Phys.* **1984**, *81*, 511−519.
(61) Nose, S. *Mol. Phys.* **1984**, *52*, 255−268.
(62) Nose, S. *Mol. Phys.* **1986**, *57*, 187−191.
(63) Plimpton, S. J. *J. Comput. Phys.* **1995**, *117*, 1.
(64) Plimpton, S. J.; Pollock, R.; Stevens, M. In *the Eighth SIAM Conference on Parallel Processing for Scientific Computing*: Minneapolis, 1997.
(65) Verlet, L. *Phys. Rev.* **1967**, *159*, 98.
(66) Hockney, R. W.; Eastwood, J. W. *Computer simulation using particles*; McGraw-Hill International Book Co.: New York, 1981.
(67) Mayo, S. L.; Olafson, B. D.; Goddard, W. A. *J. Phys. Chem.* **1990**, *94*, 8897.
(68) Li, T.; Wlaschin, A.; Balbuena, P. B. *Ind. Eng. Chem. Res.* **2001**, *40*, 4789.
(69) Jang, S. S.; Blanco, M.; Goddard, W. A.; Caldwell, G.; Ross, R. B. *Macromolecules* **2003**, *36*, 5331.
(70) Levitt, M.; Hirshberg, M.; Sharon, R.; Laidig, K. E.; Daggett, V. *J. Phys. Chem. B* **1997**, *101*, 5051.
(71) Starkweather, H. W. *Macromolecules* **1982**, *15*, 320.
(72) Moore, R. B.; Martin, C. R. *Macromolecules* **1989**, *22*, 3594.
(73) Porat, Z.; Fryer, J. R.; Huxham, M.; Rubinstein, I. *J. Phys. Chem.* **1995**, *99*, 4667.
(74) Fried, H.; Binder, K. *J. Chem. Phys.* **1991**, *94*, 8349.
(75) Molina, L. A.; Rodriguez, A. L.; Freire, J. J. *Macromolecules* **1994**, *27*, 1160.
(76) Molina, L. A.; Freire, J. J. *Macromolecules* **1995**, *28*, 2705.
(77) Hoffmann, A.; Sommer, J.-U.; Blumen, A. *J. Chem. Phys.* **1997**, *106*, 6709.
(78) Hoffmann, A.; Sommer, J.-U.; Blumen, A. *J. Chem. Phys.* **1997**, *107*, 7559.
(79) Jo, W. H.; Jang, S. S. *J. Chem. Phys.* **1999**, *111*, 1712.
(80) Binder, K. *Colloid Polym. Sci.* **1987**, *265*, 273.
(81) Sariban, A.; Binder, K. *J. Chem. Phys.* **1987**, *86*, 5859.
(82) Sariban, A.; Binder, K. *Colloid Polym. Sci.* **1987**, *265*, 424.
(83) Sariban, A.; Binder, K. *Colloid Polym. Sci.* **1988**, *266*, 389.
(84) Sariban, A.; Binder, K. *Colloid Polym. Sci.* **1989**, *267*, 469.
(85) Chakrabarti, A.; Toral, R.; Gunton, J. D.; Muthukumar, M. *J. Chem. Phys.* **1990**, *92*, 6899.
(86) Sariban, A.; Binder, K. *Macromolecules* **1991**, *24*, 578.
(87) Brown, G.; Chakrabarti, A. *Phys. Rev. E* **1993**, *48*, 3705.
(88) Brown, G.; Chakrabarti, A. *J. Chem. Phys.* **1993**, *98*, 2451.
(89) Jo, W. H.; Kim, S. H. *Macromolecules* **1996**, *29*, 7204.
(90) Jo, W. H.; Kim, J. G.; Jang, S. S.; Youk, J. H.; Lee, S. C. *Macromolecules* **1999**, *32*, 1679.
(91) Schuster, M.; Kreuer, K. D.; Maier, J. In *14th international conference on solid-state ionics*: Monterey, USA, 2003; p 395.
(92) Paddison, S. J.; Paul, R.; Kreuer, K.-D. *Phys. Chem. Chem. Phys.* **2002**, *4*, 1151.
(93) Okada, T.; Xie, G.; Meeg, M. *Electrochim. Acta* **1998**, *14*, 2141.
(94) Zawodzinski, T. A.; Springer, T. E.; Davey, J.; Jestel, R.; Lopez, C.; Valerio, J.; Gottesfeld, S. *Electrochim. Acta* **1995**, *40*, 297.
(95) Kreuer, K. D. *Solid-State Ionics* **1997**, *97*, 1.